

# Generalized gradient exchange functionals based on the gradient-regulated connection: a new member of the TCA family

Éric Brémond · Diane Pilard · Ilaria Ciofini ·  
Henry Chermette · Carlo Adamo · Pietro Cortona

Received: 19 July 2011 / Accepted: 14 October 2011 / Published online: 11 March 2012  
© Springer-Verlag 2012

**Abstract** A new type of generalized gradient approximation exchange functional coupled with the TCA correlation model has been proposed. Based on gradient-regulated connection, this exchange functional is able to mix performances of a modified PBE for the bulk region, to those of the PW91 for the asymptotic one, leading to a significant improvement on the modelization of weak interacting systems, while keeping a good accuracy for the atomization energies.

**Keywords** Exchange-correlation functional · Gradient-regulated connection · Tognetti–Cortona–Adamo functional

**Electronic supplementary material** The online version of this article (doi:10.1007/s00214-012-1184-0) contains supplementary material, which is available to authorized users.

Dedicated to Professor Vincenzo Barone and published as part of the special collection of articles celebrating his 60th birthday.

É. Brémond · D. Pilard · I. Ciofini · C. Adamo (✉)  
Laboratoire d'Électrochimie, Chimie des Interfaces et  
Modélisation pour l'Énergie, UMR 7575, Chimie ParisTech,  
11 rue P. et M. Curie, 75231 Paris Cedex 05, France  
e-mail: carlo-adamo@chimie-paristech.fr

H. Chermette  
Institut de Sciences Analytiques-Laboratoire de Chimie  
Physique Théorique, bat. Dirac, Université de Lyon, Université  
Lyon 1 and CNRS UMR 5280, 43 bd du 11 novembre 1918,  
69622 Villeurbanne Cedex, France

P. Cortona  
Laboratoire Structure, Propriété et Modélisation des Solides,  
UMR 8580, École Centrale Paris, Grande Voie des Vignes,  
92295 Châtenay-Malabry, France  
e-mail: pietro.cortona@ecp.fr

## 1 Introduction

Density functional theory (DFT) is, nowadays, probably the most widely used first principle approach, both in solid-state physics and in chemistry. The main reason is its good balance between performances (*e.g.*, accuracy in computed geometrical and electronic structure features) and computational cost. Thus, it is not surprising that both the development of new exchange-correlation functionals and their benchmarking are currently extremely flourishing, the aim being a more and more accurate description of system's properties.

Functionals are normally ranked using the Perdew ladder, which focuses on the degree of non-locality included in the functional expression [1]. In such a way, functionals are classed from strictly local, such as the local density approximation, to non-local, for example, global hybrid functionals containing a fraction of exchange computed in a Hartree-Fock fashion using Kohn-Sham orbitals. In between, there are the semi-local functionals belonging to the generalized gradient approximation (GGA) or the meta-GGA classes, which offer a compromise between accuracy and efficiency. During the last decades, a great variety of GGAs have been proposed and tested. Some of them are nowadays extremely popular: for instance, the Perdew-Wang PW86 [2] and PW91 [3] or the Perdew, Burke, and Ernzerhof (PBE) [4] functional.

Nonetheless, from their first proposal [5], global hybrid functionals marked a real breakthrough for applications to chemical systems, since they normally outperform the GGAs for thermochemical properties. Among them, B3LYP [6, 7] and PBE0 [8, 9] probably best represent the two different philosophies used to develop new hybrid functionals, which is the introduction in the functional form of fitted parameters (B3LYP) and the “parameter-free”

approach, based on the fulfillment of a number of theoretical conditions (PBE0). Indeed, if such functionals definitely changed the DFT world at molecular level, their use and implementation in codes using plane waves, that is the very large majority of codes for solid state or first principle dynamics, are still far from efficient, thus making their use often unaffordable [10].

In this context, recently, some of us proposed an exchange-correlation functional, obtained by combining the PBE exchange, which is known to lead pretty accurate estimations of atomization energies and activation barriers, with a new GGA correlation functional [11]. The latter, usually referred to as TCA, was derived by including gradient-dependent terms in the local correlation functional proposed by Ragot and Cortona [12]. Successively, a revised version of the TCA correlation functional (called revTCA) was derived [13] by taking into account a supplementary physical constraint, that is, the vanishing correlation energy of one-electron systems. The revTCA correlation, combined with a modified PBE exchange proposed by the same authors [13] (revPBE, which should not be confused with the similar, but not identical, revised PBE exchange proposed by Zhang and Yang [14]), led to a GGA exchange-correlation functional whose performances are not far from those of hybrid functionals for several properties [15, 16], thus constituting a net improvement with respect to standard GGAs. Nevertheless, this functional still fails to model weak interactions, a failure of which can be attributed to the exchange part of the functional, particularly for hydrogen-bonded systems. Since the PW91 exchange has proven to yield satisfactory results for the description of weakly interacting systems, while the PBE (or revPBE) functional provides a good description of ionic-covalent systems, it is reasonable to conceive that a new GGA exchange functional, combining PBE (or revPBE) for the description of the bulk region, that is, for small reduced gradients, and the PW91 for the asymptotic region, responsible for the modeling of a weak interaction, could overcome the limitations of the original revTCA functional.

In this paper, we focus on a possible approach, the gradient-regulated connection (GRAC) [17], allowing a smooth merge of two different exchange functionals. The resulting exchange will be combined with the revTCA correlation, which has previously proved to outperform other GGA correlation functionals for classical thermochemical benchmarks. The GRAC approach follows the same philosophy of those proposed by Pople [18], by Goddard and coworkers [19], or of that recently proposed by Truhlar [20]. However, in contrast with all these approaches where two analytical expressions for the exchange functional are mixed in a uniform way, here the ratio between the two contributions is regulated by a continuous function.

The structure of the paper is the following. After a brief description of the GRAC approach and of the computational setup, the optimal range of switching between the bulk and asymptotic regions will be investigated. Once this range defined, the properties of the newly defined GRAC-revTCA functional will be tested over a series of standard benchmark sets, also including weakly interacting systems.

## 2 Gradient-regulated connection based exchange functionals

Originally developed by Grüning et al. [17], the GRAC was proposed to correct the asymptotic behavior of an exchange potential, so as to allow the description of the bulk density region by a potential and the density tail region by another one. The link between these two potentials is made by a switching function  $f$  varying from zero (in the region where the reduced density gradient is null) to one (in the region where the reduced density gradient tends to infinity).

Using a similar approach in order to join functionals instead of potentials, the new exchange functional  $\mathfrak{F}^{b \rightarrow a}$  developed in this paper combines a first exchange functional  $\mathfrak{F}^b$ , recognized to be accurate in the bulk region, with a second one  $\mathfrak{F}^a$ , which reproduces well the asymptotic behavior:

$$\mathfrak{F}^{b \rightarrow a}[\rho(\mathbf{r})] = [1 - f[x(\mathbf{r})]] \cdot \mathfrak{F}^b[\rho(\mathbf{r})] + f[x(\mathbf{r})] \cdot \mathfrak{F}^a[\rho(\mathbf{r})] \quad (1)$$

In this equation,  $\rho$  is the electron density and  $x$  is the reduced density gradient defined by:

$$x : \mathbb{R}^3 \rightarrow [0, +\infty[ \\ \mathbf{r} \mapsto \frac{|\nabla \rho(\mathbf{r})|}{\rho(\mathbf{r})^{\frac{4}{3}}} \quad (2)$$

The switching function  $f$  is chosen to be the Fermi-like function (Fig. 1):

$$f_{\alpha, \beta}[x(\mathbf{r})] = \frac{1}{1 + \exp(-\alpha(x(\mathbf{r}) - \beta))} \quad (3)$$

where  $\alpha$  and  $\beta$  are parameters governing how the bulk and asymptotic regions are linked. In particular,  $\alpha$  regulates the switching slope, whereas  $\beta$  indicates the position of the switch region, that is, the value of the reduced density gradient for which  $\mathfrak{F}^{b \rightarrow a}$  is equal to the average of  $\mathfrak{F}^a$  and  $\mathfrak{F}^b$ .

Considering the conversion completed when  $f_{\alpha, \beta}[x(\mathbf{r})] = M$ , the functional domain can be split in three parts (Fig. 1):  $[0, \beta - \beta_s]$ ,  $[\beta - \beta_s, \beta + \beta_s]$  and  $[\beta + \beta_s, +\infty[$ , named  $b$ ,  $b \rightarrow a$ , and  $a$ , respectively. The  $\beta_s$  value is given

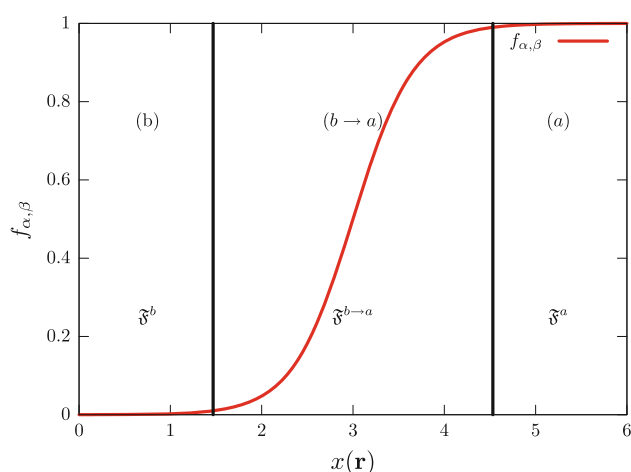


**Fig. 1** The representation of the Fermi function

by:  $\beta_s = \alpha^{-1} \cdot \ln\left(\frac{M}{1-M}\right)$ . Clearly, the steeper is the switching slope, the more the value of  $\beta_s$  tends to zero.

In order to define the  $\beta$  value, a first approach could be to use the definition of the “physical interval” given by Perdew et al. [21, 22]. Following these authors, the bulk region is restrained to the interval  $x(\mathbf{r}) \in [0, 3 \times 2 \cdot (3\pi^2)^{\frac{1}{3}}]$ . It is expected that values of  $\beta$  not too different from this one do not produce significant modifications of the results. Similarly, as  $\alpha$  determine how quickly the switch from one exchange to the other is done, its precise value should not influence too much the results, if the switch region is not too large.

### 3 Computational details

The GRAC exchange functional was implemented in the GAUSSIAN Development Version [23], including its analytical first to third derivatives. The correlation functional was always fixed to revTCA [13]. Several reference datasets were used in order to analyze the behavior in function of the  $\alpha$  and  $\beta$  parameters of the Fermi function and to assess the performances of the resulting exchange-correlation functional. The result changes in function of the  $\alpha$  and  $\beta$  values were studied by computing the mean absolute error (MAE) for the atomization energies of the G2-148 dataset [24] and for the NCB31 test set [25]. The latter is a dataset that was especially conceived in order to test the functional performances for systems characterized by weak interactions. For both datasets, the Pople’s triple- $\zeta$  basis set 6-311+G(3df, 2p) was used.

The performances of the so obtained GRAC-revTCA method were compared with those of standard GGA exchange functionals (PBE [4], revPBE [13], PW91 [3]) using the same revTCA correlation counterpart, and to

those of the global hybrid PBE0 [8, 9], considered here as a reference for the performances of hybrid functionals.

The performances of all the above mentioned functionals were tested on barrier heights (from the DBH24/08 test set [26, 27]), weak interactions (from the NCB31 dataset [25]), structural parameters (from the G2-32 set [28]), or hydrogen-bond length optimizations and dissociation energies (from the HB10 bench test [28]). As described in literature, systems belonging to the DBH24/08 test set were described by a 6-31+G(*d*, *p*) basis set.

For the HB10 database, structures were fully optimized using 6-311+G(3df, 2p) basis set, while dissociation energies were computed using the larger Dunning quadruple- $\zeta$  basis set aug-cc-pVQZ, in order to minimize the error due to the basis set superposition (BSSE).

Finally, all the calculations were performed using a tight criterion for the self-consistent field (SCF) convergence and a standard integration grid.

## 4 Results and discussions

### 4.1 Analysis of the influence of the $\alpha$ and $\beta$ parameter values

Let us start by considering the atomization energies of the G2-148 dataset. As previously discussed, on the basis of the “physical interval” concept introduced by Perdew and coworkers [21, 22], reasonable values of  $\beta$  should be close to  $3 \times 2 \cdot (3\pi^2)^{\frac{1}{3}} \approx 18.6$ . Let us set  $\beta = 19$  and study the influence of  $\alpha$ .

In Fig. 2 are reported the enhancement functions  $F(s)$  of the original revPBE and PW91 exchange functionals as well as the GRAC-revTCA  $F(s)$  for different  $\alpha$  values. The matching of the functionals is very smooth for  $\alpha = 0.5$  and

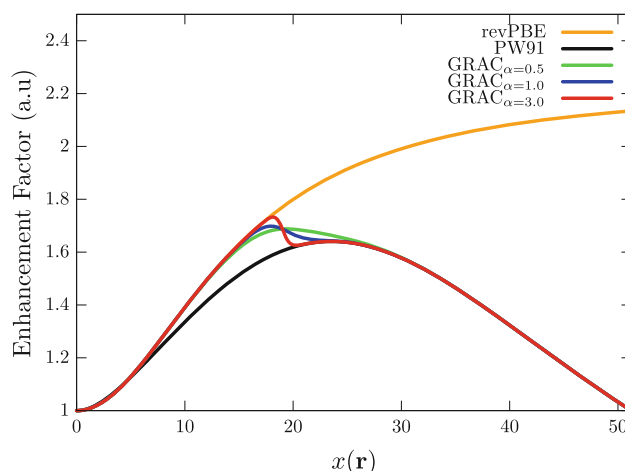


**Fig. 2** The representation of the revPBE, PW91, and GRAC functional for  $\beta$  equal to 19 and different values of  $\alpha$

becomes progressively sharp (but always keeping a “regular” character in mathematical sense) increasing the  $\alpha$  value. Variations of the  $\alpha$  value within the interval  $\alpha \in [1.0, 4.5]$  produce MAE changes smaller than  $0.5 \text{ kcal mol}^{-1}$ .

A second piece of information is obtained by studying the MAE in function of  $\alpha$  and  $\beta$ . The latter is assumed to vary in an interval of values around  $\beta \approx 18.6$ . The results are reported in Fig. 3, where it can be seen that the MAE surface, in a quite large range of the parameter values ( $\alpha \in [1.0, 4.5]$ ,  $\beta \in [17.5, 19.5]$ ), is indeed flat. There is no MAE minimum in this region (for a reason that will become clear in the following), and the flat character of the surface actually means that any pair of values could be arbitrarily chosen with only minor consequences on the results.

A further, important, piece of information is obtained by studying the MAE changes in a largest range of  $\beta$  values for a fixed value of  $\alpha$  ( $\alpha = 1$ ). The results of this study, for both the G2-148 and the NCB31 datasets, are reported in Fig. 4. This figure confirms some known features of the parents functionals and furnishes some interesting new

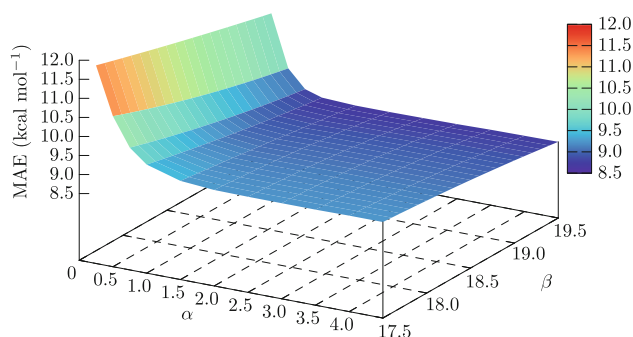


**Fig. 3** Mean average error (MAE) surface for the atomization energy of the G2-148 test set function of the  $\alpha$  and  $\beta$  parameters

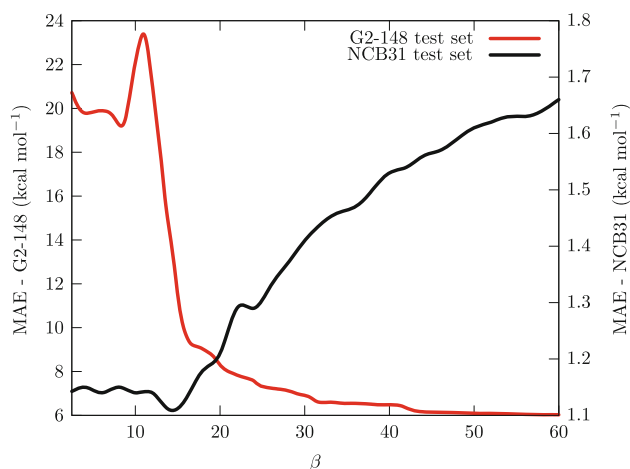


**Fig. 4** Cross section of the three dimensional surface ( $\alpha$ ,  $\beta$ , MAE) at  $\alpha = 1$  of the G2-148 and NCB31 test sets as a function of the  $\beta$  parameter

insights. Increasing the weight of the revPBE exchange (that is increasing the  $\beta$  value) improves the G2-148 atomization energies, while the description of the weak interactions worsens. The contrary happens reducing the  $\beta$  value. A more surprising result is that relatively high values of the reduced gradient are still important for the calculation of the atomization energies. The revPBE exchange seems to be (when combined with the revTCA correlation) the optimum one on the overall range of the reduced gradient values. Thus, any choice of the  $\beta$  value will give rise to a G2-148 MAE greater than the one of the parent revPBE functional. However, our aim is to improve the description of weakly interacting systems, keeping the errors for the atomization energies reasonably low. Figure 4 shows that this can be done by choosing  $\beta$  on the basis of the “physical interval” concept. Changes of its value, within a range that can be deduced by inspection of Fig. 4, have the only consequence of slightly improving the results for one dataset at the expense of the other. For this reason, the choice of the  $\beta$  value is relatively arbitrary.

Our calculations have been performed by setting  $\beta = 19$  and  $\alpha = 1$ . This latter value corresponds to  $\beta_s \approx 2.9$  and was chosen in order to have a  $F(s)$  function as smooth as possible, keeping the transition from one exchange to the other sufficiently fast. Thus, the GRAC-revTCA functional used in the following has mainly a revPBE character for  $x(\mathbf{r}) \in [0, 16]$ , a PW91 character for  $x(\mathbf{r}) \in [22, +\infty[$ , while the interval  $x(\mathbf{r}) \in [16, 22]$  can be considered the switching region.

## 4.2 Benchmarks

The performances of the above defined GRAC-revTCA functional were tested on different databases and compared to those of PBE-revTCA, PW91-revTCA, revPBE-revTCA, PBE0, and the GRAC0-revTCA functional. The last one is obtained by using the same  $\alpha$  and  $\beta$  parameter values as in the GRAC-revTCA case, but the PBE exchange functional in the bulk region instead of revPBE, that is  $\mathcal{E}^{\text{PBE} \rightarrow \text{PBE}}$  instead of  $\mathcal{E}^{\text{revPBE} \rightarrow \text{PBE}}$  as used for GRAC-revTCA.

The main results are summarized in Fig. 5, while detailed information for each database is reported in the Supporting Information.

### 4.2.1 Atomization energies and structural optimizations

The atomization energy datasets, G2-X (with X equal to the number of molecules), are the reference test sets routinely used both to optimize the functional parameters (if any) and to assess the functional performances [29].

Analyzing the results obtained for the G2-148 set, it appears that the PBE0 global hybrid is just slightly better

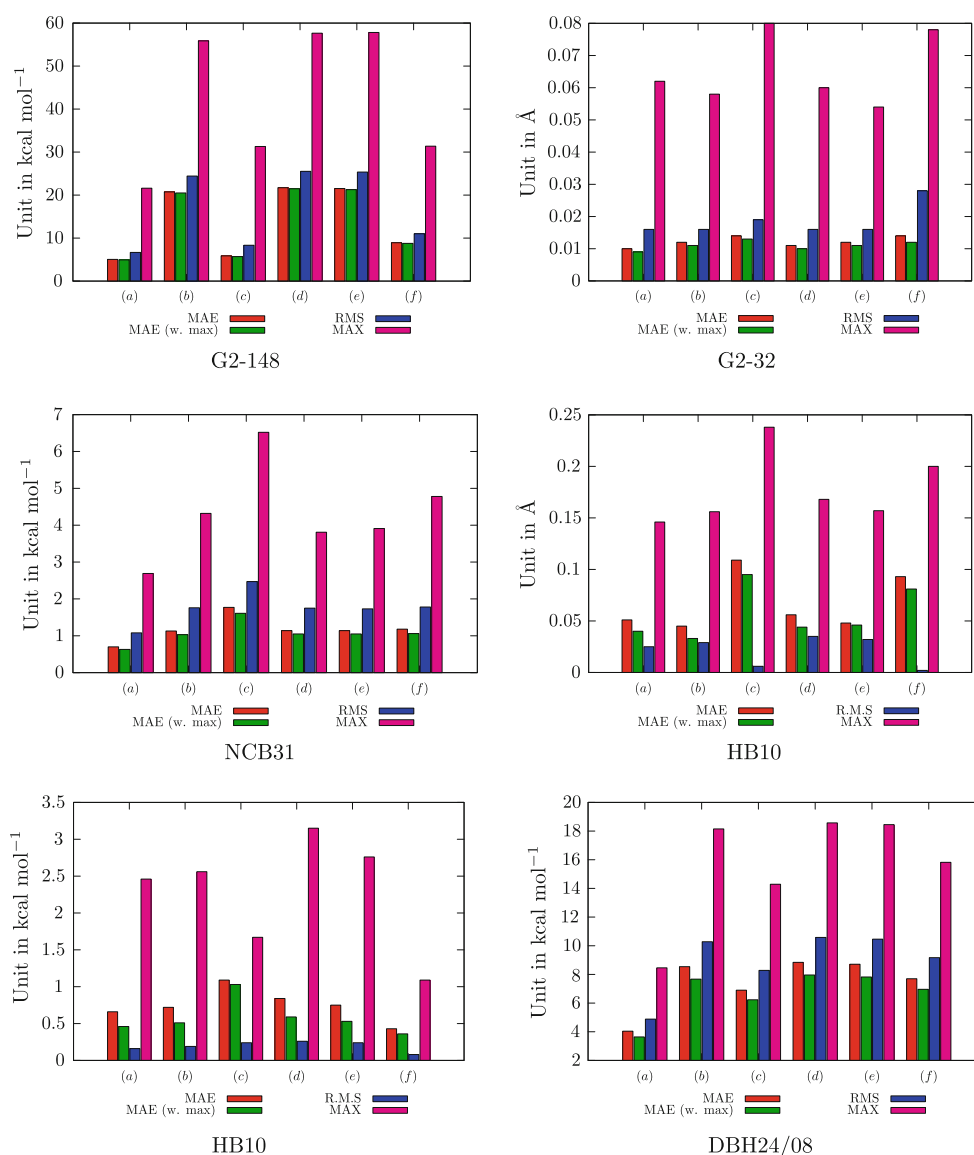


**Fig. 5** Histogram representation of the error computed on different test sets. (a) PBE0, (b) PBE-revTCA, (c) revPBE-revTCA, (d) PW91-revTCA, (e)  $\tilde{\gamma}^{\text{revPBE} \rightarrow \text{PBE}}$ -revTCA (GRAC0-revTCA), (f)  $\tilde{\gamma}^{\text{revPBE} \rightarrow \text{PBE}}$ -revTCA (GRAC-revTCA)

than the revPBE-revTCA GGA functional (the MAE is 0.8 kcal mol<sup>-1</sup> smaller). The performances of both are clearly better than those of all the other GGA exchange functionals (PBE, PW91) coupled with the revTCA correlation. The GRAC-revTCA functional provides a satisfactory MAE, intermediate between that of revPBE-revTCA and PW91-revTCA, of only 8.9 kcal mol<sup>-1</sup>, while a much higher MAE (21.5 kcal mol<sup>-1</sup>) is computed for GRAC0-revTCA. These results follow the evolution of the error computed going from revPBE-revTCA to PBE-revTCA and thus clearly underly the importance of the use of the revPBE exchange functional instead of the PBE one in conjunction with the revTCA correlation.

The second test set, G2-32, was used to evaluate the performances of the different functionals for structural optimizations. Actually, all functionals show a very similar behavior. The computed MAE is always lower than 0.02 Å, and the differences among the various functionals being smaller than 0.004 Å. In the case of the GRAC-revTCA, the worst result is obtained for the Li<sub>2</sub> compound.

#### 4.2.2 Weak interactions

The first dataset we have used, in order to test the new functional on weakly bonded systems, was the NCB31 one. This dataset is composed of 31 “dimers”, that is, six



hydrogen-bonding dimers (HB6), seven charge transfer complexes (CT7), six dipole interaction complexes (DI), seven weak-interaction pairs (WI7), and five  $\pi$ - $\pi$  stacking complexes (PPS5). Since the GRAC-revTCA functional was devised in order to improve the results for this kind of systems, we expect better performances with respect to those of revPBE-revTCA. This is actually the case: the MAE is reduced from 1.8 kcal mol<sup>-1</sup> for revPBE-revTCA, to 1.2 kcal mol<sup>-1</sup> for GRAC-revTCA, very close to the values computed for the PW91-revTCA (1.14 kcal mol<sup>-1</sup>), and the PBE-revTCA (1.13 kcal mol<sup>-1</sup>) functionals. Although the errors are still larger than those obtained at the PBE0 level (0.70 kcal mol<sup>-1</sup>), the accuracy is satisfactory for a pure GGA functional.

The HB10 dataset, containing ten hydrogen-bonded molecular complexes, was used for a second benchmark. Again the better performances of the GRAC exchange functional, with respect to the parent revPBE, both on energetics and structural features, are clearly demonstrated by our results. Indeed, the mean errors on H-bond optimized distances are still roughly 0.04 Å larger than those obtained at PBE0 or PBE-revTCA level. On the other hand, energetic features are greatly improved with respect to all the other functionals, and the GRAC-revTCA errors on the dissociation energies being two times smaller than those of PBE0, a more than satisfactory result for a GGA functional.

#### 4.2.3 Reaction barriers

Finally, in order to test the behavior of the different functionals on reaction barriers and, consequently, on chemical kinetics, the DBH24/08 dataset was used. This set is composed by 24 barriers, corresponding to 12 different reactions, including hydrogen transfer (HT), heavy atom transfer (HAT), nucleophilic substitution (NS), and unimolecular and association (UA) reactions. The performances of the GRAC-revTCA functional are better than those of PBE-revTCA, PW91-revTCA, or GRAC0-revTCA, but slightly worst than those of the parent revPBE-revTCA functional. For barriers, the best results are obtained by using the hybrid PBE0 functional, whose MAE is only 4.0 kcal mol<sup>-1</sup>, to be compared with 7.7 kcal mol<sup>-1</sup> for GRAC-revTCA.

## 5 Conclusion

A new exchange functional was designed to allow, when coupled with the GGA revTCA correlation, a balanced description of both ionic-covalent and weak interacting systems. The main idea is to combine two different exchange functionals in such a way that their strengths are kept and their weaknesses are reduced. A similar idea has

been followed by other authors [30, 31] in order to derive functionals, which give good performances simultaneously for molecules and solids.

The new functional is based on the gradient-regulated connection, with the link between the functionals describing the bulk and the asymptotic regions regulated by a Fermi function, in analogy to the original GRAC approach. The revPBE exchange functional, which provides results for atomization energies having an accuracy close to that of hybrid functionals, was used in the bulk region, while the PW91 one, reputed for its performances on weakly interacting systems, was chosen for the asymptotic region. The values of the two parameters, required to define the Fermi switch function, can be chosen quite arbitrarily in a relatively large region with only minor consequences on the results.

The functional obtained (GRAC-revTCA) has good performances for thermochemistry. For example, the MAE for the G2 dataset is better than those of the PBE-TCA approximation [11], which, in turn, reduces the errors of the PBE-PBE functional approximately by a factor of two. It is interesting to notice that this performance is similar to that of the recently proposed SOGGA11 approximation [20]. This is an empirical functional, and its ability to calculate atomization energies was tested by using the MGAE109/05 dataset [32], obtaining a MAE smaller than the PBE one for a factor of about two. We emphasize that the main strength of the GRAC-revTCA functional is its ability to describe weak interactions, keeping a good accuracy for properties of ionic-covalent systems. The results for hydrogen bonds are indeed very good, displaying improved performances even with respect to a hybrid functional such as PBE0.

Work is in progress to analyze more in details the best way of tailoring the enhancement function  $F(s)$ , eventually enabling the use of more than two exchange-correlation functionals to better describe all reduced density gradient domains.

## 6 Supporting informations

Detailed data on the G2-148, G2-32, NCB31, HB10, and DBH24 dataset as well as MAE maps computed for the NCB31 set.

**Acknowledgments** This work was funded by the ANR agency under the project DinFDFT ANR 2010 BLANC n. 0425, and by Sanofi-Aventis.

## References

1. Perdew JP, Ruzsinszky A, Constantin LA, Sun J, Csonka GI (2009) J Chem Theory Comput 5:902–908

2. Perdew JP (1986) *Phys Rev B* 33:8822–8824
3. Perdew JP, Wang Y (1992) *Phys Rev B* 45:13244–13249
4. Perdew JP, Burke K, Ernzerhof M (1996) *Phys Rev Lett* 77:3865–3868
5. Becke AD (1992) *J Chem Phys* 96:2155–2160
6. Becke AD (1993) *J Chem Phys* 98:5648–5652
7. Barone V, Adamo C (1994) *Chem Phys Lett* 224:432–438
8. Adamo C, Barone V (1999) *J Chem Phys* 110:6158–6170
9. Ernzerhof M, Scuseria GE (1999) *J Chem Phys* 110:5029–5037
10. Guidon M, Schiffmann F, Hutter J, VandeVondele J (2008) *J Chem Phys* 128:214104
11. Tognetti V, Cortona P, Adamo C (2008) *J Chem Phys* 128:034101
12. Ragot S, Cortona P (2004) *J Chem Phys* 121:7671–7680
13. Tognetti V, Cortona P, Adamo C (2008) *Chem Phys Lett* 460:536–539
14. Zhang Y, Yang W (1998) *Phys Rev Lett* 80:890
15. Tognetti V, Cortona P, Adamo C (2009) *Theor Chim Acta* 122:257–264
16. Tognetti V, Adamo C, Cortona C (2010) *Inter Sci* 2:163–168
17. Grüning M, Gritsenko OV, van Gisbergen SJA, Baerends EJ (2001) *J Chem Phys* 114:652–660
18. Adamson RD, Gill PMW, Pople JA (1998) *Chem Phys Lett* 284:6
19. Xin X, Zhang Q, Muller RP, Goddard WA (2005) *J Chem Phys* 122:014105
20. Peverati R, Zhao Y, Truhlar DG (2011) *Phys Chem Lett* 2:1991–1997
21. Zupan A, Burke K, Ernzerhof M, Perdew JP (1997) *J Chem Phys* 106:10184–10193
22. Zupan A, Perdew JP, Burke K, Causà M (1997) *Int J Quant Chem* 61:835–845
23. Frisch MJ et al (2010) Gaussian DV, revision H.10. Gaussian, Inc., Wallingford, CT
24. Johnson BG, Gill PMW, Pople JA (1993) *J Chem Phys* 98:5612–5626
25. Zhao Y, Schultz NE, Truhlar DG (2006) *J Chem Theory Comp* 2:364–382
26. Zheng J, Zhao Y, Truhlar DG (2009) *J Chem Theory Comp* 5:808–821
27. Lynch BJ, Truhlar DG (2003) *J Phys Chem A* 107:8996–8999
28. Boese AD, Martin JML (2004) *J Chem Phys* 121:3405–3416
29. Adamo C, Barone V (1998) *J Chem Phys* 108:664–675
30. Haas P, Tran F, Schwarz K (2011) *Phys Rev B* 83:205117
31. Fabiano E, Constantin LA, Della Sala F (2010) *Phys Rev B* 82:113104
32. Zhao Y, Schultz NE, Truhlar DG (2005) *J Chem Theory Comput* 2:364–382